Available online at www.sciencedirect.com
ScienceDirect
Trans. Nonferrous Met. Soc. China 25(2015) 1439−1445
Transactions of Nonferrous Metals Society of China
www.tnmsc.cn

Microstructures and mechanical properties of as-extruded and heat treated Mg−6Zn−1Mn−4Sn−1.5Nd alloy

Guang-shan HU[1,2], Ding-fei ZHANG[1,2], Yu-feng DONG[1,2], Xia CHEN[1,2], Lu-yao JIANG[1,2], Fu-sheng PAN[1,2]

1. College of Materials Science and Engineering, Chongqing University, Chongqing 400045, China;
2. National Engineering Research Center for Magnesium Alloys, Chongqing University, Chongqing 400044, China

Received 9 June 2014; accepted 11 December 2014

Abstract: The microstructures and mechanical properties of Mg−6Zn−1Mn−4Sn−1.5Nd alloy subjected to extrusion and T5 treatment were investigated using optical microscopy (OM), X-ray diffractometer (XRD), scanning electron microscopy (SEM), electron back scattered diffraction (EBSD), transmission electron microscopy (TEM), hardness tests and uniaxial tensile tests. The results showed that the as-cast alloy consisted of α(Mg), Mn, Mg_7Zn_3, Mg_2Sn and MgSnNd phases. Dynamic recrystallization has completed during the extrusion process and the average grain size was 7.2 μm. After T5 treatment, the strength increased obviously, the yield strength and ultimate tensile strength of as-extruded alloy were increased by 94 and 34 MPa, respectively. Microstructure characterization revealed that the improvement of strength was determined by the high number density of β'_1 rods.
Key words: Mg−6Zn−1Mn−4Sn−1.5Nd alloy; extrusion; T5 heat treatment; microstructures; mechanical properties

1 Introduction

In recent years, magnesium (Mg) alloys have attracted great attention due to their low density, high specific strength, good castability and excellent machinability [1−3]. The applications of wrought Mg alloys in automotive and aerospace industries produce substantial weight reduction and fuel efficiency increment [4]. However, poor formability and strength at room temperature limited their applications. Therefore, the development of high strength and high plasticity wrought Mg alloys is necessary.

Mg−Zn−Sn alloys are typical age-hardenable wrought Mg alloys, which have great potential to improve the strength by various heat treatments and alloying [5]. The precipitation sequence of Mg−Zn−Sn alloys is SSSS (supersaturated solid solution)→G.P. zone (discs, globular or band)→β'_1 ($MgZn_2$ or Mg_4Zn_7) →β'_2 ($MgZn_2$,) →β' (Mg_2Sn)→β (Mg_2Zn_3 or MgZn) [5−9]. The β'_1, β'_2 and β' precipitates are strengthening phases. When β phase is formed, over-aging occurs and the mechanical properties decrease. ZHANG et al [8,9] and ZHAO et al [10] have developed a promising high strength Mg−6Zn−1Mn−4Sn (mass fraction, %) (ZMT614) wrought alloy (all compositions are in mass fraction unless specially stated). T6 treatment ((440 °C, 2 h) + (180 °C, 8 h)) markedly improves the strength of as-extruded ZMT614 alloy.

In addition, previous investigations have reported that the mechanical properties of Mg−Zn−Sn alloys were improved by the addition of Al, Ag, Li and Nd elements [11−14]. The addition of such alloying elements could enhance age hardening response and improve mechanical properties. Nd, as one of rare-earth elements, could refine the grains and form new phases in Mg alloys. NING et al [11] have reported that a minor addition of Nd enhanced the strength of Mg−0.3Zn−0.32Zr wrought alloy for the fine grains and tiny Mg_{12}(Nd,Zn) precipitates within the grains and along the grain boundaries.

Based on the previous investigations, we have developed a new high strength Mg−6Zn−1Mn−4Sn−1.5Nd (ZMT614−1.5Nd) wrought alloy. Up to now, there have been limited investigations on its microstructures and mechanical properties in the hot extrusion and heat treatment conditions. Therefore, the aim of this work is to investigate the microstructural

Foundation item: Project (2013CB632200) supported by the National Great Theoretic Research, China; Project (2011BAE22B01-3) supported by the National Sci & Tech Support Program, China; Project (2010DFR50010) supported by the International Cooperation, Sharing Fund of Chongqing University's Large-scale Equipment, China
Corresponding author: Ding-fei ZHANG; Tel: +86-23-65112491; E-mail: zhangdingfei@cqu.edu.cn
DOI: 10.1016/S1003-6326(15)63743-8

evolution and mechanical properties of as-extruded and T5-treated ZMT614−1.5Nd alloy.

2 Experimental

Billets with a diameter of 80 mm were prepared by a ZG−0.01 vacuum induction melting furnace under an Ar atmosphere. The chemical composition of Mg−6.03Zn−0.94Mn−4.0Sn−1.59Nd (denoted as ZMT614−1.5Nd) was tested using an XRF−1800 CCDE sequential X-ray fluorescence spectrometer. The as-cast ingots were homogenized at 420 °C for 12 h. After homogenization, the ingots were hot extruded into bars of 16 mm in diameter at 420 °C with the extrusion ratio of 25:1 and followed by cooling in air. Then, the as-extruded samples were aged at 180 °C (T5) for several hours.

Tensile tests were carried on a SANS CMT−5105 electronic universal testing machine at room temperature. Samples for tensile tests had a cross-sectional diameter of 5 mm and a gauge length of 50 mm. The strain rate of samples was 1×10^{-3}/s. The yield strength, ultimate tensile strength and elongation to fracture were averaged over three samples. Phase components were characterized by a Rigaku D/max 2500PC X-ray diffractometer (XRD) using Cu K_{α}. The microstructures were observed by an LEXT 4000 laser metallographic microscope (OM). The microstructural morphology and compound compositions of the alloys were examined using an ESCAN VEGAⅡ scanning electron microscope (SEM) equipped with an oxford INCA Energy 350 energy dispersive X-ray spectrometer (EDS). Electron back scattered diffraction (EBSD) analysis was performed by using a JEOL−7001F scanning electron microscope equipped with TSL OIM Analysis 5 software. Transmission electrical microscope (TEM) observations were made using a JEOL JEM−2100 microscope operated at 200 kV. The TEM specimens were prepared by the precision ion polishing system (MODEL 1010).

3 Results and discussion

3.1 Microstructures of as-cast and homogenized alloy

Figure 1 shows the XRD pattern of the as-cast ZMT614−1.5Nd alloy. The phase compositions of the as-cast sample are α(Mg), Mn, Mg_7Zn_3, Mg_2Sn and MgSnNd phases. For the Mg−Zn−Nd alloys, when the mass ratio of Zn/Nd is between 3 and 5, $Mg_7Zn_{11}Nd_2$ phase is formed. However, $Mg_7Zn_{11}Nd_2$ phase is not found in this alloy. Thermodynamic calculations provide a promising way to predict the forming ability of metallic compounds. A phase is more prone to form and its stability is better when its formation enthalpy is smaller. According to Miedema and extrapolation models [15], the formation enthalpies of Mg_7Zn_3, Mg_2Sn, MgSnNd and $Mg_7Zn_{11}Nd_2$ phases is −3.5, 9.7, −50.7 and −17.3 kJ/mol, respectively. The formation enthalpy of MgSnNd phase is much smaller than that of the other phases. As a result, the MgSnNd phase is preferred to form firstly.

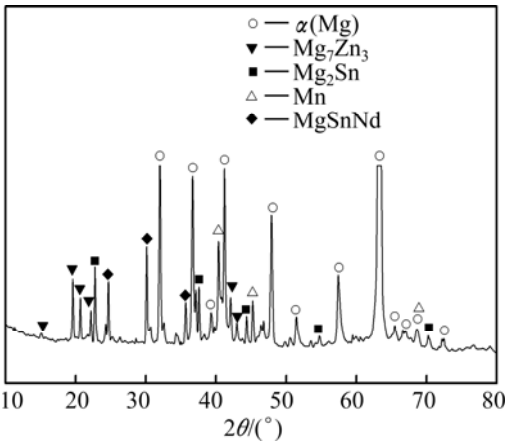

Fig. 1 XRD pattern of as-cast alloy

Figure 2 shows the microstructures of as-cast and as-homogenized ZMT614−1.5Nd alloys. The as-cast alloy exhibits a typical dendritic structure with α(Mg) matrix and intermetallic compounds in interdendritic regions (Fig. 2(a)). BSE (backscatter electron) image shows that the intermetallic compounds contain continuous gray and isolated bright phases. According to the EDS analysis, the chemical compositions of continuous compounds are 73.45% Mg and 26.55% Zn (mole fraction), while those of isolated compounds are 56.85% Mg, 27.19% Sn and 15.96% Nd. Combined with the XRD analysis, the continuous compounds are Mg_7Zn_3 phase and the isolated compounds are MgSnNd and Mg_2Sn mixed phases. After homogenization, most of the eutectic phases dissolve into the matrix while the cluster compounds are remained. The remained compounds are MgSnNd and Mg_2Sn phases identified by the EDS analysis, suggesting that they are high temperature phases.

3.2 Microstructures of as-extruded alloy

Figure 3 shows the microstructures of as-extruded samples. Dynamic recrystallization (DRX) occurs and the grains get refined. The average grain size is 7.2 μm. The remained compounds are broken into various dimension particles and distribute as streamlines parallel to the extrusion direction. EDS analysis reveals that the chemical compositions of Mg, Sn and Nd of the point *A* are 35.20%, 34.62% and 30.18% (mole fraction), respectively, and the n(Mg)/n(Sn)/n(Nd) ratio is approximately 1:1:1, which is approved as the MgSnNd

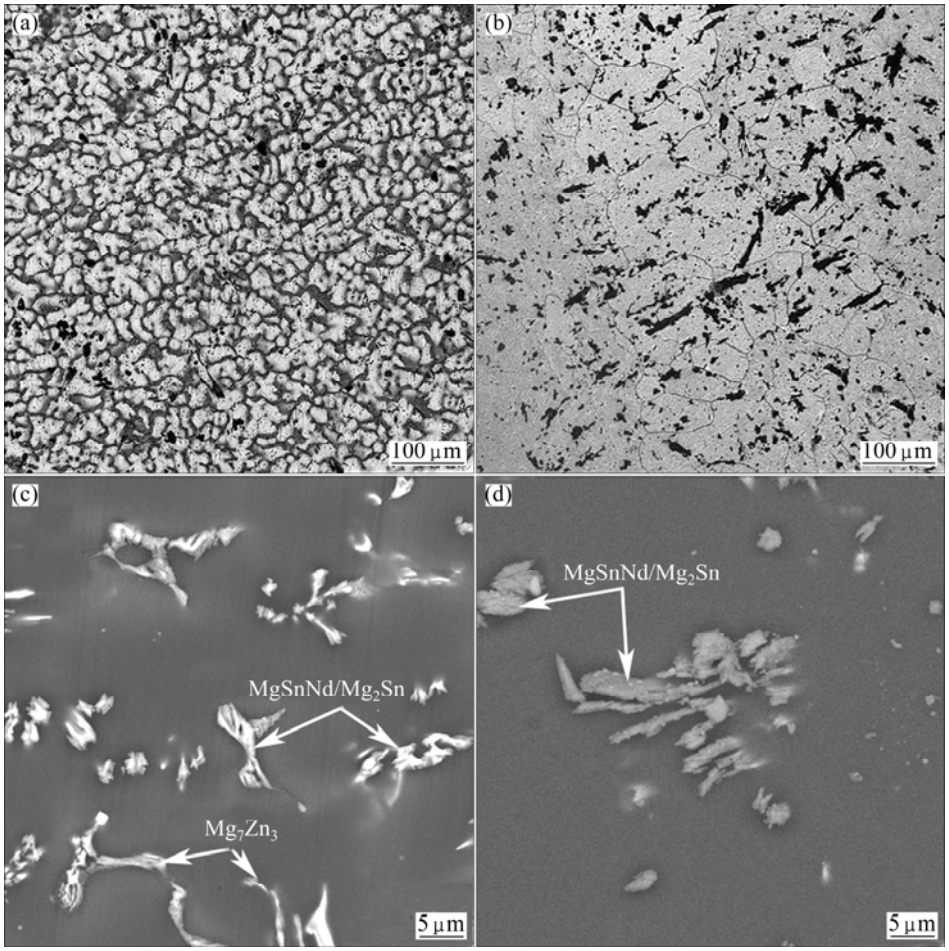

Fig. 2 Microstructures of as-cast and as-homogenized alloys: (a) Optical micrograph of as-cast sample; (b) Optical micrograph of as-homogenized sample; (c) BSE image of as-cast sample; (d) BSE image of as-homogenized sample

phase combined with the XRD results. A small number of rod-shaped and sphere-shaped particles disperse in the grains and at the boundaries randomly. The rods should be β'_1 phase precipitated in the air cooling process [16]. The sphere-shaped phase may be β'_2 or Mg_2Sn phase.

In order to illustrate the microstructural evolution precisely during the extrusion, EBSD analysis was used. Figure 4 shows the inverse pole figure (IPF) and pole figures (PFs) of the cross-section of the as-extruded sample. Different colors indicate different crystallographic orientations in IPF map. DRX has completed and grains growth occurs in the extrusion, which are consistent with the optical microstructures. Several coarse grains whose sizes are over 15 μm lie in the matrix. The PFs exhibit high intensity texture along the circumference in the (0001) PF, while the highlights are at the center of $(10\bar{1}0)$ PF. It is a typical basal fiber texture of as-extruded Mg alloys. Exactly, the basal plane is aligned along the extrusion direction [17,18]. The maximum intensity of extrusion texture is only 3.824, suggesting that the effect of this texture on the mechanical properties of as-extruded alloy is small.

3.3 Microstructures of as-aged alloy

Figure 5 shows the variation in hardness of ZMT614−1.5Nd alloy as functions of aging time at 180 °C. The peak hardness is obtained at 12 h. The peak hardness is HV 81.5, which is about HV 9 higher than the initial hardness. As the aging time increases further, over aging occurs and the hardness decreases. Figure 6 shows the XRD pattern of peak aged alloy. It reveals that the dissolved Zn element precipitates again and $MgZn_2$ phase forms. The peak aged sample consists of α(Mg), Mn, $MgZn_2$, Mg_2Sn and MgSnNd phases.

Figure 7 shows the bright field TEM (BF-TEM) and corresponding fast Fourier transform (FFT) patterns of ZMT614−1.5Nd alloy under peak aged state. All images are obtained from $[11\bar{2}0]_\alpha$ zone axis. Three types of phases disperse in the peak aged alloy. One is the coarse polygonal-shaped MgSnNd phase, another is the fine Mg_2Sn phase. The MgSnNd and Mg_2Sn phases are high temperature phases and are undissolved during the homogenization. Then, they are broken into different shapes in the following extrusion. Consequently, these phases are not precipitated and their morphologies are

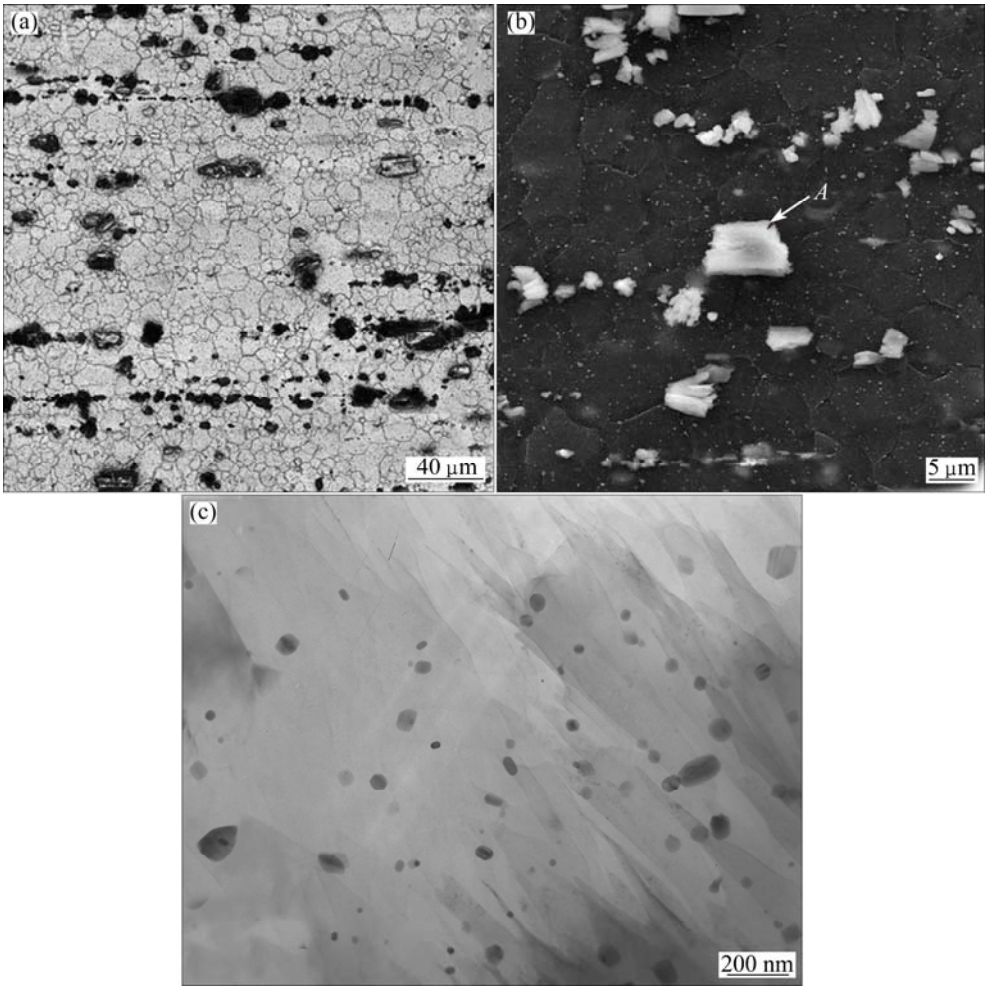

Fig. 3 Microstructures of as-extruded alloy: (a) Optical micrograph; (b) SEM image; (c) TEM image

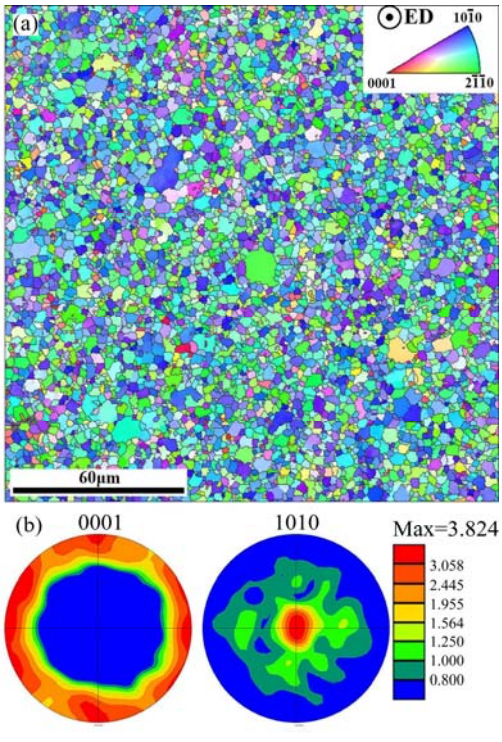

Fig. 4 IPF (a) and PFs (b) microstructures of as-extruded alloy

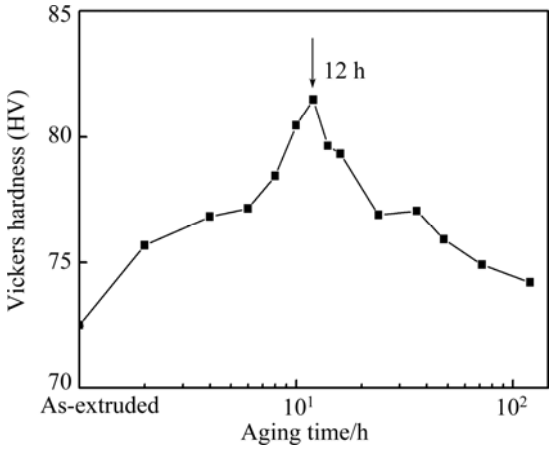

Fig. 5 Variation in hardness as function of aging time of T5-treated alloy

not changed in the T5 treatment. The third is the fine rod-shaped phase, which is parallel to $[0001]_\alpha$ zone axis. By the previous investigations and XRD analysis [6−19], we conclude that the rods are β_1' phase. The number density of β_1' rods is much higher than that of as-extruded alloy. Through the FFT pattern, it can be

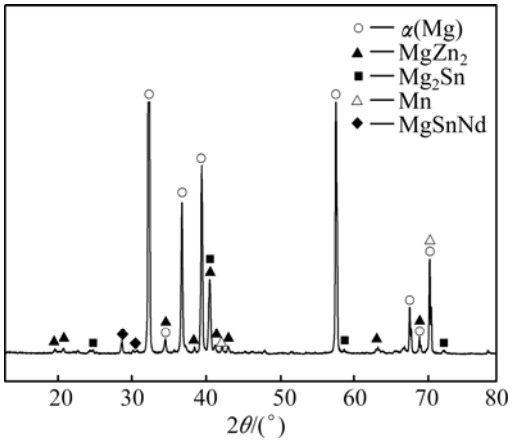

Fig. 6 XRD pattern of peak aged alloy

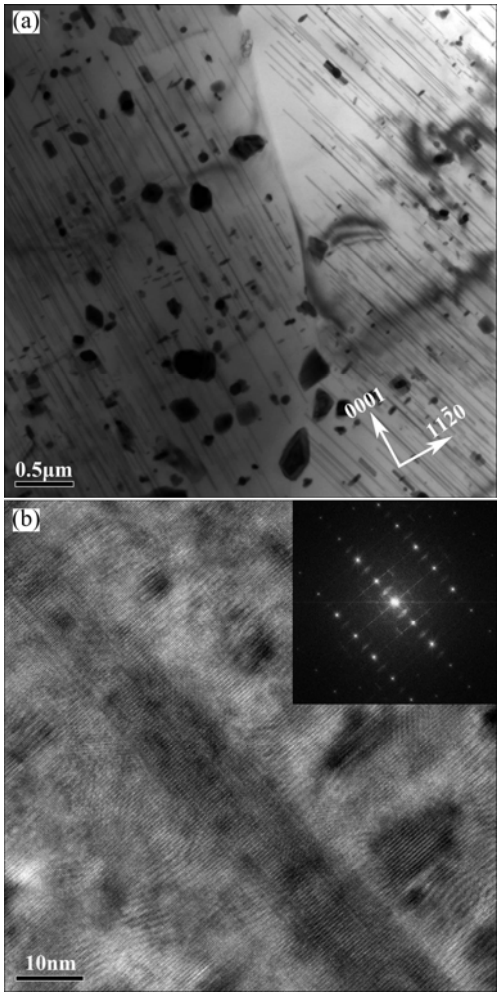

Fig. 7 TEM images and corresponding FFT pattern of peak aged alloy: (a) BF-TEM image obtained from $[11\bar{2}0]_{Mg}$ zone axis; (b) HR-TEM image of rod-like β_1' phase (inset: corresponding FFT pattern)

seen that the β_1' phase is coherent with the matrix and its orientation relationship is $[0001]_{\beta_1'}//[11\bar{2}0]_{\alpha}$ and $(11\bar{2}0)_{\beta_1'}//(0001)_{\alpha}$. Therefore, the rod-shaped β_1' precipitate can act as a more enormous impediment to the motion of dislocations than the other phases in the deformation [20].

3.4 Mechanical properties

The tensile properties of as-extruded and as-aged alloys are shown in Fig. 8. Compared with the as-extruded sample, T5 treatment remarkably enhances the ultimate tensile strength (UTS) and yield strength (YS). The elongation appears to somewhat decrease. It decreases from 11.36% to 10.12%. For the peak aged alloy, the UTS and YS are 364 and 338 MPa, which are respectively 34 and 94 MPa higher than that of the as-extruded sample, and are superior to the typical high strength wrought Mg alloys such as ZK60 and AZ31.

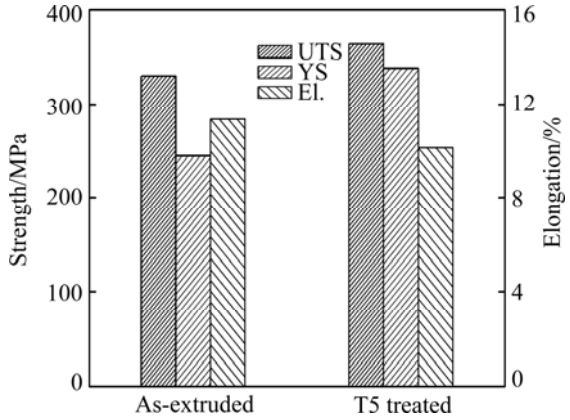

Fig. 8 Tensile properties of as-extruded and peak aged alloys

The improvement of YS is attributed to the grain boundary strengthening, solid solution strengthening and precipitation strengthening [20,21]. Based on the Orowan looping mechanism, ZHU and STARKE [22] and LIU et al [23] have established a widely used model to estimate the precipitation strengthening of rod-shaped precipitates at room temperature.

$$\sigma_{ppt}=0.12\frac{MGb}{\sqrt{Ad^2}}(f_v^{\frac{1}{2}}+0.70A^{\frac{1}{2}}f_v+0.12Af_v^{\frac{1}{2}})\cdot \ln(\frac{0.158Ad}{4b}) \quad (1)$$

where σ_{ppt} is the contribution of precipitation strengthening, M is the Taylor factor, G is shear modulus of the Mg matrix, b is the magnitude of the Burgers vector, A is the aspect ratio of the rods, d is the mean diameter and f_v is the volume fraction of the precipitates. It is supposed that all the rod-shaped β_1' precipitates have the same morphology in the as-extruded and as-aged alloys. Then, Eq. (1) can be rewritten as

$$\sigma_{ppt}=Kf_v^n \quad (2)$$

where K and n are constants. Equation (2) suggests that the precipitation strengthening is proportional to the

volume fraction of rod-shaped β_1' phase. From Fig. 3(c) and Fig. 7(a), the number density of β_1' precipitates substantial increases in the peak aged state, leading to the increment of strength obviously. In addition, the coarse MgSnNd particles may act as crack initiation and makes the strength decrease in the deformation. However, the precipitation strengthening plays the dominating role in the enhancement of strength for the as-aged alloys compared with the as-extruded ZMT614−1.5Nd alloy.

4 Conclusions

1) The as-cast alloy consists of α(Mg), Mn, $MgZn_2$, Mg_2Sn and MgSnNd phases.

2) DRX has been completed and grain growth occurs during the extrusion. The average grain size is about 7.2 μm.

3) High number density of β_1' rods precipitate in the T5 treatment process. The β_1' rods are parallel to the $[0001]_\alpha$ zone axis and its orientation relationship is $[0001]_{\beta_1'}//[11\bar{2}0]_\alpha$ and $(11\bar{2}0)_{\beta_1'}//(0001)_\alpha$.

4) Compared with the as-extruded alloy, the UTS and YS of T5-treated alloy are increased by 34 and 94 MPa, respectively.

References

[1] GAO L, YAN H, LUO J, ALAN A, CHEN R S. Microstructure and mechanical properties of a high ductility Mg−Zn−Mn−Ce magnesium alloy [J]. Journal of Magnesium and Alloys, 2013, 1(4): 283−291.

[2] DONG Yun, LIN Xiao-ping, YE Jie, ZHENG Run-guo, HE Na. Microstructure of Mg−8Zn−4Al−1Ca aged alloy [J]. Transactions of Nonferrous Metals Society of China, 2014, 24(2): 310−315.

[3] WANG L, QIAO Q, LIU Y, SONG X. Formability of AZ31 Mg alloy sheets within medium temperatures [J]. Journal of Magnesium and Alloys, 2013, 1(4): 312−317.

[4] NIE J F. Precipitation and hardening in magnesium alloys [J]. Metallurgical and Materials Transactions A, 2012, 43(11): 3891−3939.

[5] OH-ISHI K, HONO K, SHIN K S. Effect of pre-aging and Al addition on age-hardening and microstructure in Mg−6.0wt% Zn alloys [J]. Materials Science and Engineering A, 2008, 496(1−2): 425−433.

[6] TAKAHASHI Y, KOJIMA K. Study of precipitates in an aged Mg−3.6 wt% Zn alloy by an X-ray method [J]. Institute of Light Metals, 1973, 23: 376−382.

[7] WANG Ying-dong, WU Guo-hua, LIU Wen-cai, PANG Song, ZHANG Yang, DING Wen-jiang. Influence of heat treatment on microstructures and mechanical properties of gravity cast Mg−4.2Zn−1.5RE−0.7Zr magnesium alloy [J]. Transactions of Nonferrous Metals Society of China, 2013, 23(12): 3611−3620.

[8] QI F G, ZHANG D F, ZHANG X H, XU X X. Effect of Sn addition on the microstructure and mechanical properties of Mg−6Zn−1Mn (wt.%) alloy [J]. Journal of Alloys and Compounds, 2014, 585: 656−666.

[9] SHI Guo-liang, ZHANG Ding-fei, ZHANG Hong-ju, ZHAO Xia-bing, QI Fu-gang, ZHANG Kui. Influence of pre-deformation on age-hardening response and mechanical properties of extruded Mg−6%Zn−1%Mn alloy [J]. Transactions of Nonferrous Metals Society of China, 2013, 23(3): 586−592.

[10] ZHAO Xian-feng, LI Shu-bo, WANG Qing-feng, DU Wen-bo, LIU Ke. Effects of heat treatment on microstructure and mechanical properties of Mg−5Zn−0.63Er alloy [J]. Transactions of Nonferrous Metals Society of China, 2013, 23(1): 59−65.

[11] NING Z L, WANG H, LIU H H, CAO F Y, WANG S T, SUN J F. Effects of Nd on microstructures and properties at the elevated temperature of a MGg−0.3Zn−0.32Zr alloy, Mater Design, 2010, 31: 4438−4444.

[12] HUANG X F, ZHANG W Z. Improved age-hardening behavior of Mg−Sn−Mn alloy by addition of Ag and Zn [J]. Materials Science and Engineering A, 2012, 552: 211−221.

[13] YANG M B, QIN C Y, PAN F S, ZHOU T. Comparison of effects of cerium, yttrium and gadolinium additions on as-cast microstructure and mechanical properties of Mg−3Sn−1Mn magnesium alloy [J]. Journal of Rare Earths, 2011, 29(6): 550−557.

[14] WANG Jun, ZHU Xiu-rong, XU Yong-dong, WANG Rong, NIE Jing-jiang, ZHANG Li-jun. Effect of rare-earth Ce and Y on microstructure and mechanical properties of AZ80 Mg alloys [J]. The Chinese Journal of Nonferrous Metals, 2014, 24(1): 25−35. (in Chinese)

[15] OUYANG Y F, ZHONG X P, DU Y, JIN Z P, HE Y H, YUAN Z H. Formation enthalpies of Fe−Al−RE ternary alloys calculated with a geometric model and Miedema's theory [J]. Journal of Alloys and Compounds, 2006, 416(1−2): 148−154.

[16] PARK S S, OH Y S, KANG D H, KIM N J. Microstructural evolution in twin-roll strip cast Mg−Zn−Mn−Al alloy [J]. Materials Science and Engineering A, 2007, 449: 352−355.

[17] OH-ISHI K, MENDIS C L, HOMMA T, KARMADO S, OHKUBO T, HONO K. Bimodally grained microstructure development during hot extrusion of Mg−2.4Zn−0.1Ag−0.1Ca−0.16 Zr (at.%) alloys [J]. Acta Materialia, 2009, 57(18): 5593−5604.

[18] BORKAR H, GAUYIN R, PEKGULERYUZ M. Effect of extrusion temperature on texture evolution and recrystallization in extruded Mg−1%Mn and Mg−1%Mn−1.6%Sr alloys [J]. Journal of Alloys and Compounds, 2013, 555: 219−224.

[19] RASHKOVA B, PRANTL W, GORGL R, KECHES J, COHEN S, BAMBERGER M, DEHM G. Precipitation processes in a Mg−Zn−Sn alloy studied by TEM and SAXS [J]. Materials Science and Engineering A, 2008, 494(1−2): 158−165.

[20] NIE J F. Effects of precipitate shape and orientation on dispersion strengthening in magnesium alloys [J]. Scripta Materialia, 2003, 48(8): 1009−1015.

[21] ZHANG L, GONG M, PENG L M. Microstructure and strengthening mechanism of a thermomechanically treated Mg−10Gd−3Y−1Sn−0.5Zr alloy [J]. Materials Science and Engineering A, 2013, 565: 262−268.

[22] ZHU A W, STARKE J E A. Strengthening effect of unshearable particles of finite size: A computer experimental study [J]. Acta Materialia, 1999, 47(11): 3263−3269.

[23] LIU G, ZHANG G J, DING X D, SUN J, CHEN K H. Modeling the strengthening response to aging process of heat-treatable aluminum alloys containing plate/disc- or rod/needle-shaped precipitates [J]. Materials Science and Engineering A, 2003, 344(1): 113−124.

挤压态和热处理态 Mg−6Zn−1Mn−4Sn−1.5Nd 镁合金的显微组织和力学性能

胡光山[1,2]，张丁非[1,2]，董于凤[1,2]，谌 夏[1,2]，蒋璐瑶[1,2]，潘复生[1,2]

1. 重庆大学 材料科学与工程学院，重庆 400045；2. 重庆大学 国家镁合金材料工程技术研究中心，重庆 400044

摘 要：利用光学显微镜、X 射线衍射仪、扫描电镜、电子背散射衍射、透射电镜、硬度以及力学性能测试等对挤压态和 T5 处理态的 Mg−6Zn−1Mn−4Sn−1.5Nd 镁合金的显微组织和力学性能进行研究。研究结果表明：合金铸态的相组成为 α(Mg)、Mn、Mg_7Zn_3、Mg_2Sn 和 MgSnNd 相。挤压过程中完成动态再结晶，再结晶晶粒的平均尺寸为 7.2 μm。T5 热处理显著提高挤压态合金的强度。合金的屈服强度和抗拉强度分别增加 94 MPa 和 34 MPa。显微组织分析表明，合金强度的提高主要是由于时效过程中析出高密度的 β'_1 杆状相。

关键词：Mg−6Zn−1Mn−4Sn−1.5Nd 合金；挤压；T5 热处理；显微组织；力学性能

(Edited by Yun-bin HE)